

ammonium head group of the surfactant. This seems to favor a water structure driven attraction between micelles. The attractive component of the intermicellar potential becomes dominant at high surfactant concentrations, where monomeric surfactant acts as a background electrolyte, screening electrostatic repulsions between micelles. Competition between the attractive and repulsive components of the intermicellar potential leads to

a high critical volume fraction of micelles.

*Acknowledgment.* We acknowledge the help of M. Dubois and P. Lixon with the analysis of the surfactants, that of I. Barnes and L. Auvray with the SANS experiments, and also L. Belloni for his assistance with the theoretical modeling of these micellar solutions.

## Photosensitized Electron-Transfer Reactions and H<sub>2</sub> Evolution in Organized Microheterogeneous Environments: Separation of Ground-State Xanthene-Bipyridinium Complexes by SiO<sub>2</sub> Colloids

I. Willner,\* Y. Eichen, and E. Joselevich

Department of Organic Chemistry and Fritz Haber Center for Molecular Dynamics Research, The Hebrew University of Jerusalem, Jerusalem 91904, Israel (Received: July 13, 1989; In Final Form: October 25, 1989)

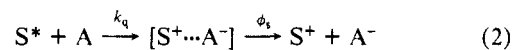
Rose bengal, Rb<sup>2-</sup>, forms a ground-state complex with *N,N'*-dimethyl-4,4'-bipyridinium, MV<sup>2+</sup>, with an association constant of  $K_a = 11000 \pm 1100 \text{ M}^{-1}$ . Static electron-transfer quenching of excited Rb<sup>2-</sup> occurs in the complex structure, but charge separation is eliminated due to rapid back electron transfer in the encounter cage complex of photoproducts. In the presence of added SiO<sub>2</sub> colloid particles the [Rb<sup>2-</sup>...MV<sup>2+</sup>] complex is separated through the selective association of MV<sup>2+</sup> to the negatively charged colloid interface. Upon illumination of a solution that includes Rb<sup>2-</sup>, MV<sup>2+</sup>, and the sacrificial electron donor triethanolamine (TEOA) in the presence of SiO<sub>2</sub> colloid, the photosensitized formation of MV<sup>•+</sup> proceeds effectively,  $\phi = 0.1$ . Mechanistic studies reveal that TEOA reduces excited Rb<sup>2-</sup> in the primary electron-transfer process. The intermediate photoproducts, TEOA<sup>•+</sup> and Rb<sup>•-</sup>, are stabilized against back-electron-transfer reactions by means of electrostatic interactions with the SiO<sub>2</sub> interface, leading to the electrical repulsion of Rb<sup>•-</sup> from the colloid interface. The control of the recombination process of the intermediate photoproducts leads to the subsequent effective reduction of MV<sup>2+</sup>. A xanthene dye-bipyridinium complex is also formed between eosin, Eo<sup>2-</sup>, and *N,N'*-dibenzyl-3,3'-dimethyl-4,4'-bipyridinium, BMV<sup>2+</sup>,  $K_a = 17000 \pm 3400 \text{ M}^{-1}$ . The complex is separated by a SiO<sub>2</sub> colloid that is immobilized with Pd metal catalyst sites. Separation of the complex allows charge separation and subsequent H<sub>2</sub> evolution (or hydrogenation of ethylene) upon illumination of the microheterogeneous assembly in the presence of TEOA. Mechanistic studies show that the SiO<sub>2</sub> colloid controls the photoinduced electron-transfer process, and stabilization of the intermediate photoproducts against the back-electron-transfer process is achieved.

Photosensitized electron-transfer reactions (eq 1) provide a general route for the conversion of light energy into chemical potential.<sup>1-3</sup> Numerous examples of the subsequent utilization



of the redox products in H<sub>2</sub> evolution,<sup>4-6</sup> CO<sub>2</sub> reduction,<sup>7-9</sup> hydrogenation of unsaturated substrates,<sup>10,11</sup> regeneration of natural

cofactors and subsequent biotransformations,<sup>12-14</sup> and NO<sub>3</sub><sup>-</sup> fixation<sup>15</sup> have been reported in recent years. The photosensitized electron-transfer process from the light absorbent, S, to an electron acceptor, A, is limited by the electron-transfer quenching efficiency and separation yield of the primary encounter cage complex of photoproducts (eq 2). Subsequently, the back-electron-transfer process of the separated photoproducts (eq 3) degrades the energy



stored by the photoproducts and limits the yield of usable redox products. Various organized microenvironments composed of micelles,<sup>16-18</sup> liposomes,<sup>19,20</sup> polyelectrolytes,<sup>21</sup> charged colloids,<sup>22,23</sup>

(1) *Energy Resources Through Photochemistry and Catalysis*; Grätzel, M., Ed.; Academic Press: New York, 1983.

(2) *Photochemical Conversion and Storage of Solar Energy*; Connolly, J. S., Ed.; Academic Press: New York, 1981.

(3) (a) Bard, A. J. *Science (Washington, D.C.)* **1980**, *207*, 1380. (b) Grätzel, M. *Acc. Chem. Res.* **1981**, *14*, 376. (c) Willner, I.; Steinberger-Willner, B. *Int. J. Hydrogen Energy* **1988**, *13*, 593.

(4) *Photogeneration of Hydrogen*; Harriman, A., West, M. E., Eds.; Academic Press: London, 1983.

(5) (a) Sutin, N.; Creutz, C. *Pure Appl. Chem.* **1980**, *52*, 2717. (b) Keller, P.; Moradpour, A.; Amouyal, E. *J. Chem. Soc., Faraday Trans. 1* **1982**, *78*, 3331.

(6) (a) Grätzel, M.; Kalyanasundaram, K.; Kiwi, J. *Struct. Bonding (Berlin)* **1982**, *49*, 37. (b) Kirch, M.; Lehn, J.-M.; Sauvage, J.-P. *Helv. Chim. Acta* **1979**, *62*, 1345. (c) Krishnan, C. V.; Sutin, N. *J. Am. Chem. Soc.* **1981**, *103*, 2141.

(7) (a) Hawecker, J.; Lehn, J.-M.; Ziessel, R. *Helv. Chim. Acta* **1986**, *69*, 1990. (b) Lehn, J.-M.; Ziessel, R. *Proc. Natl. Acad. Sci. U.S.A.* **1982**, *79*, 701.

(8) (a) Maidan, R.; Willner, I. *J. Am. Chem. Soc.* **1986**, *108*, 8100. (b) Maidan, R.; Willner, I. *J. Am. Chem. Soc.* **1986**, *108*, 1080. (c) Willner, I.; Maidan, R.; Mandler, D.; Dürr, H.; Dörr, G.; Zengerle, K. *J. Am. Chem. Soc.* **1987**, *109*, 6080.

(9) (a) Mandler, D.; Willner, I. *J. Am. Chem. Soc.* **1987**, *109*, 7884. (b) Mandler, D.; Willner, I. *J. Chem. Soc., Perkin Trans. 2* **1988**, 997.

(10) Degani, Y.; Willner, I. *J. Chem. Soc., Perkin Trans. 2* **1986**, 37.

(11) Mandler, D.; Willner, I. *J. Phys. Chem.* **1987**, *91*, 3600.

(12) Mandler, D.; Willner, I. *J. Chem. Soc., Chem. Commun.* **1986**, 851.

(13) Mandler, D.; Willner, I. *J. Chem. Soc., Perkin Trans. 2* **1986**, 805.

(14) Willner, I.; Mandler, D. *Enzyme Microb. Technol.* **1989**, *11*, 467.

(15) Lapidot, N.; Riklin, A.; Willner, I. *J. Am. Chem. Soc.* **1989**, *111*, 1883.

(16) (a) Fendler, J. H. *Chem. Rev.* **1987**, *87*, 877. (b) Matsuo, T.; Takama, K.; Tsutsui, Y.; Nishizima, T. *J. Coord. Chem. Rev.* **1980**, *10*, 195.

(17) (a) Kalyanasundaram, K. *Chem. Soc. Rev.* **1978**, *7*, 453. (b) Turro, N. J.; Grätzel, M.; Braun, A. M. *Angew. Chem., Int. Ed. Engl.* **1980**, *19*, 675. (c) Thomas, J. K. *Chem. Rev.* **1980**, *80*, 283.

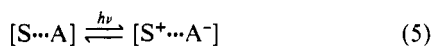
(18) (a) Kurihara, K.; Fendler, J. H.; Ravet, I.; Nagy, J. *J. Mol. Catal.* **1986**, *34*, 325. (b) Meyer, M.; Wallberg, L.; Kurihara, K.; Fendler, J. H. *J. Chem. Soc., Chem. Commun.* **1984**, 90.

(19) Kurihara, K.; Sukigara, M.; Toyoshima, Y. *Biochem. Biophys. Res. Commun.* **1979**, *88*, 320.

(20) (a) Sudo, Y.; Toda, F. *Nature (London)* **1979**, *279*, 807. (b) Ford, W. E.; Otvos, J. W.; Calvin, M. *Nature (London)* **1978**, *274*, 507. (c) Ford, W. E.; Otvos, J. W.; Calvin, M. *Proc. Natl. Acad. Sci. U.S.A.* **1979**, *76*, 3590.

or microemulsions<sup>24</sup> have been designed to control vectorial electron-transfer reactions, i.e., improve the electron-transfer quenching, assist the charge separation, and retard the back-electron-transfer reactions. In these systems electrostatic and/or hydrophilic-hydrophobic interactions between the redox products and the organized microenvironment result in controlling effects on the photosensitized electron-transfer process.

Frequently,<sup>25</sup> formation of ground-state photosensitizer-electron acceptor complexes (eq 4) is a further limitation in photosensitized electron-transfer reactions. Formation of such donor-acceptor complexes results in static electron-transfer quenching of the excited photosensitizer. Although the quenching process is efficient, the resulting encounter complex of photoproducts is stabilized by interactions similar to those operative in the ground state, and consequently, rapid recombination in the cage structure takes place (eq 5). Previous studies have exemplified that mi-



celles<sup>26</sup> and cyclodextrin<sup>27</sup> receptors can be used as microenvironments that effect the separation of such photosensitizer-acceptor assemblies. In these systems selective association of one of the complex components to the micellar interface or to the cyclodextrin receptor cavity by means of electrostatic or hydrophilic interactions results in the complex dissociation. Here we wish to report on the formation of ground-state complexes between xanthene dyes and bipyridinium salts as electron acceptors.<sup>28</sup> We demonstrate the effects of SiO<sub>2</sub> colloids on the separation of these complexes and highlight the possibility of driving effective photosensitized electron-transfer reactions and subsequent H<sub>2</sub> evolution in the microheterogeneous organized environment.

### Experimental Section

*N,N'*-Dibenzyl-3,3'-dimethyl-4,4'-bipyridinium, BMV<sup>2+</sup>, was prepared by the reaction of 3,3'-dimethyl-4,4'-bipyridine with benzyl bromide. A 500-mg (2.7-mmol) sample of 3,3'-dimethyl-4,4'-bipyridine was added to 10 mL of benzyl bromide. The mixture was refluxed under argon atmosphere for 10 h. After cooling, acetone was added to the mixture until a white precipitation appeared. The white precipitate was filtered and washed three times with acetone (yield 75%). The product gave satisfactory elementary analysis.

All other reagents of the highest purity were of commercial source (Aldrich or Sigma) and were used without further purification. The colloidal SiO<sub>2</sub> (1%) was prepared by diluting a commercial 14.5% SiO<sub>2</sub> colloid (50-Å particle diameter, surface area 600 m<sup>2</sup>·g<sup>-1</sup>, particle concentration 1.7 × 10<sup>-8</sup> M; Nalco Chemical Co., Oak Brook, IL).

Absorption spectra were recorded with a Uvikon 860 (Kontron) spectrophotometer. Emission spectra were obtained with a Uvikon

SFM 25 fluorimeter. Flash photolysis experiments were performed with a DL 200 (Moletron) dye laser pumped by a UV-14 (Moletron) nitrogen laser, and the traces were recorded on a 2430A Tektronix digital oscilloscope. Hydrogen analysis was performed by gas chromatography (HP 5890) using a 5A-MS column, thermal conductivity detector, and argon as carrier gas. Ethane analysis was performed on a Tracor 540 gas chromatograph using a Porapak T-column, a flame ionization detector, and nitrogen as carrier gas.

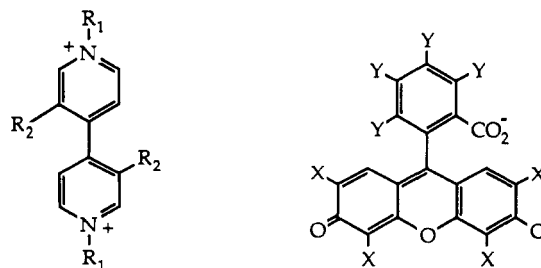
Redox potentials of BMV<sup>2+</sup> and Rb<sup>2+</sup> were measured with a BAS CV-27 cyclic voltammograph. Electrochemical experiments were performed in 0.1 N phosphate buffer aqueous solution (pH = 6.5) using paraffin oil-carbon paste electrode (BAS) as working electrode and Ag/AgCl as reference electrode. Continuous illuminations were performed with a 250-W xenon arc lamp. (Light was filtered through a Kodak 2C filter, λ > 400 nm, and infrared radiation was filtered through a CuSO<sub>4</sub> filter.) The incident photon flux was determined by Reinecke salt actinometry<sup>29</sup> to be (1.7 ± 0.5) × 10<sup>-3</sup> einstein·L<sup>-1</sup>·min<sup>-1</sup>. Size, shape, and elementary composition of Pd/SiO<sub>2</sub> colloids were determined with a Jeol 200 CX electron microscope combined with a Link 860.

Continuous illumination experiments were performed in a glass cuvette equipped with a stopper and stirring bar. For MV<sup>2+</sup> reduction experiments, samples that included 1% SiO<sub>2</sub> aqueous colloid (3 mL), TEOA (1 × 10<sup>-3</sup> M), Rb<sup>2+</sup> (1 × 10<sup>-5</sup> M), and MV<sup>2+</sup> (1 × 10<sup>-3</sup> M), pH = 9.3, were illuminated under argon atmosphere. The systems were not buffered to eliminate high ionic strength and reduction of the surface potential of the SiO<sub>2</sub> colloid. No changes in the pH of the systems were detected during the course of illumination. Sodium chloride (0, 0.005, 0.01, 0.05, and 0.1 M) was added to the systems to vary ionic strength. Hydrogen and ethane evolution experiments were performed in similar cuvettes containing 1% SiO<sub>2</sub> colloid suspensions (3 mL) that included TEOA (1 × 10<sup>-3</sup> M), eosin Y, Eo<sup>2+</sup> (1 × 10<sup>-5</sup> M), BMV<sup>2+</sup> (1 × 10<sup>-3</sup> M), and Pd(NO<sub>3</sub>)<sub>2</sub>·2H<sub>2</sub>O (1.3 × 10<sup>-6</sup> M) (pH = 9.3). Every 10–15 min, 100-μL gas samples were withdrawn for gas analysis. All the experiments were performed after flushing the cuvettes with argon for 30 min. Hydrogenation of ethylene was performed through injection of ethylene (500 μL) into the gaseous phase (2 mL) of the H<sub>2</sub> evolution photosystem.

Back-electron-transfer reactions and electron-transfer quenching were followed by means of laser flash photolysis experiments. For electron-transfer quenching of Rb<sup>2+</sup> by TEOA, an aqueous solution (pH = 9.3) that included Rb<sup>2+</sup> (1 × 10<sup>-5</sup> M) in the presence and absence of 1% SiO<sub>2</sub> colloid was flashed at λ = 440 nm at different TEOA concentrations, and the lifetime of triplet Rb<sup>2+</sup> was followed at λ = 630 nm. Back-electron-transfer processes were followed in aqueous solutions (pH = 9.3) that included TEOA (1 × 10<sup>-3</sup> M) and Rb<sup>2+</sup> (1 × 10<sup>-5</sup> M) in the absence and presence of 1% SiO<sub>2</sub> colloid. Excitation of the system was at λ = 440 nm; Rb<sup>3+</sup> was followed at λ = 415 nm.

### Results and Discussion

*Complex Formation between Rose Bengal and Methylviologen.* Addition of *N,N'*-dimethyl-4,4'-bipyridinium, methylviologen, MV<sup>2+</sup> (1), to an aqueous solution of rose bengal, Rb<sup>2+</sup> (2), results



- 1 (MV<sup>2+</sup>): R<sub>1</sub> = CH<sub>3</sub>; R<sub>2</sub> = H  
 3 (BMV<sup>2+</sup>): R<sub>1</sub> = CH<sub>2</sub>Φ; R<sub>2</sub> = CH<sub>3</sub>  
 4 (BV<sup>2+</sup>): R<sub>1</sub> = CH<sub>2</sub>Φ; R<sub>2</sub> = H  
 2 (Rb<sup>2+</sup>): X = I; Y = Cl  
 5 (Eo<sup>2+</sup>): X = Br; Y = H

(21) (a) Kelder, S.; Rabani, J. *J. Phys. Chem.* **1981**, *85*, 1637. (b) Meisel, D.; Matheson, M.; Rabani, J. *J. Am. Chem. Soc.* **1978**, *100*, 117.

(22) (a) Willner, I.; Degani, Y. *J. Chem. Soc., Chem. Commun.* **1982**, 761. (b) Laane, C.; Willner, I.; Otvos, J. W.; Calvin, M. *Proc. Natl. Acad. Sci. U.S.A.* **1981**, *78*, 5928. (c) Degani, Y.; Willner, I. *J. Am. Chem. Soc.* **1983**, *105*, 6228.

(23) (a) Furlong, D. N.; Johansen, O.; Launikonis, A.; Loder, J. W.; Mav, A. W.-H.; Sasse, W. H. *F. Aust. J. Chem.* **1985**, *38*, 363. (b) Willner, I.; Otvos, J. W.; Calvin, M. *J. Am. Chem. Soc.* **1981**, *103*, 3202. (c) Willner, I.; Yang, J.-M.; Otvos, J. W.; Calvin, M. *J. Phys. Chem.* **1981**, *85*, 3277.

(24) (a) Willner, I.; Ford, W. E.; Otvos, J. W.; Calvin, M. *Nature (London)* **1979**, *280*, 830. (b) Atik, S. S.; Thomas, J. K. *J. Am. Chem. Soc.* **1981**, *103*, 367, 7403. (c) Mandler, D.; Degani, W.; Willner, I. *J. Phys. Chem.* **1984**, *88*, 4366.

(25) (a) Brugger, P. A.; Grätzel, M.; Guarr, T.; McLendon, G. *J. Phys. Chem.* **1982**, *86*, 944. (b) Okura, I.; Kusunoki, S.; Aono, S. *Inorg. Chim. Acta* **1983**, *77*, 99. (c) Shelnut, J. A. *J. Am. Chem. Soc.* **1981**, *103*, 4275. (d) Usui, Y.; Misawa, H.; Sakuragi, H.; Tokumora, K. *Bull. Chem. Soc. Jpn.* **1987**, *60*, 1573.

(26) Willner, I.; Degani, Y. *J. Phys. Chem.* **1985**, *89*, 5685.

(27) Adar, E.; Degani, Y.; Goren, Z.; Willner, I. *J. Am. Chem. Soc.* **1986**, *108*, 4696.

(28) Usui, Y.; Misawa, H.; Sakuragi, H.; Tokumara, K. *Bull. Chem. Soc. Jpn.* **1987**, *60*, 1573.

(29) Wenger, E. E.; Adamson, A. W. *J. Am. Chem. Soc.* **1966**, *88*, 394.

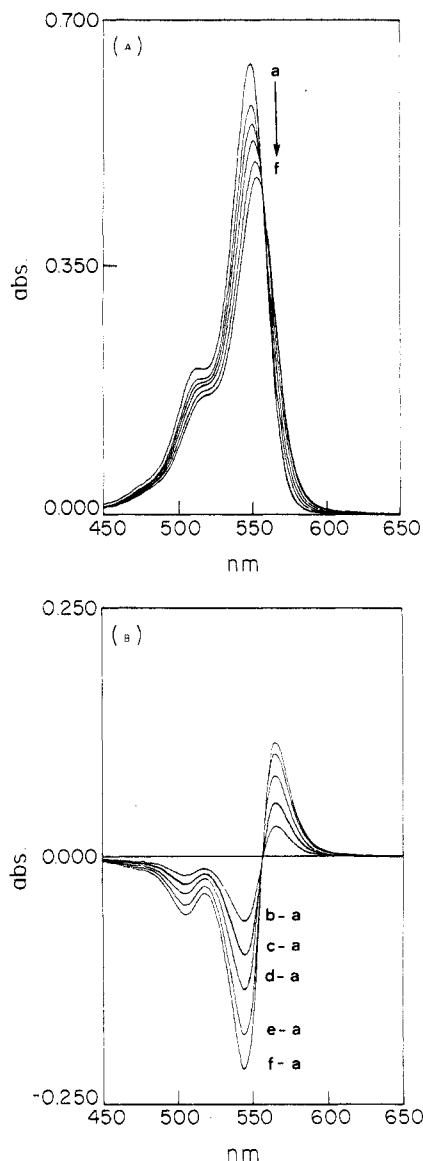
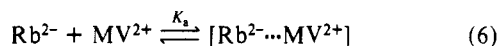


**Figure 1.** Absorption spectra (A) and differential absorption spectra (B) of rose bengal ( $5.9 \times 10^{-6}$  M) in the presence of methylviologen: (a) 0, (b)  $2.65 \times 10^{-5}$ , (c)  $5.9 \times 10^{-5}$ , (d)  $1.06 \times 10^{-4}$ , (e)  $2.12 \times 10^{-4}$ , and (f)  $3.7 \times 10^{-4}$  M.

in the formation of a dye-acceptor complex. The formation of the complex can be followed spectroscopically (Figure 1). It is evident that an isosbestic point is formed upon addition of  $MV^{2+}$  to the dye solution, implying the formation of a 1:1 complex (eq 6). From the changes in the absorption spectra of the dye at



different  $MV^{2+}$  concentrations, the association constant of the complex<sup>30</sup> is determined to have a value of  $K_a = 11000 \pm 1100$  M<sup>-1</sup>.

The formation of the dye-electron acceptor complex can also be followed by the fluorescence quenching process of the dye. Figure 2A shows the fluorescence intensity decrease of rose bengal upon addition of  $MV^{2+}$ . It is reasonable to assume that static quenching of the excited dye occurs in the complex structure and that the observed fluorescence at different  $MV^{2+}$  concentrations originates only from noncomplexed dye. If one uses this assumption, the fluorescence intensity,  $F$ , at any electron acceptor concentration (when  $[MV^{2+}] \gg [Rb^{2+}]$ ) will be given by eq 7,

$$F_0/F = K_a[MV^{2+}]; \quad [MV^{2+}] \gg [Rb^{2+}] \quad (7)$$

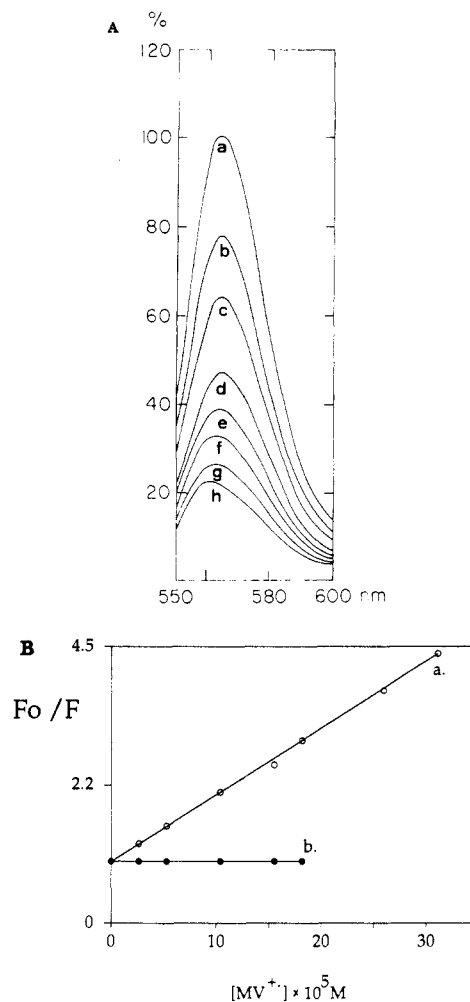


**Figure 2.** (A) Emission spectra of rose bengal ( $5.9 \times 10^{-6}$  M) in the presence of methylviologen: (a) 0, (b)  $2.6 \times 10^{-5}$ , (c)  $5.2 \times 10^{-5}$ , (d)  $1.04 \times 10^{-4}$ , (e)  $1.56 \times 10^{-4}$ , (f)  $1.82 \times 10^{-4}$ , (g)  $2.6 \times 10^{-4}$ , and (h)  $3.12 \times 10^{-4}$  M. (B) Stern-Volmer plot for the fluorescence quenching of rose bengal by  $MV^{2+}$ : (a) in the absence of  $SiO_2$  colloid; (b) in the presence of 1% w/w  $SiO_2$  colloid.

where  $F_0$  is the fluorescence intensity of the dye in the absence of quencher and  $K_a$  is the association constant of the formed complex (eq 6). Figure 2B shows the plot of  $F_0/F$  vs the concentration of  $MV^{2+}$ . A linear relationship is indeed observed, and the derived association constant corresponds to  $K_a = 10800 \pm 1100$  M<sup>-1</sup> in excellent agreement with the value derived by the spectrophotometric method. The formation of the  $[Rb^{2+} \cdots MV^{2+}]$  complex is attributed to electrostatic attraction of the bipyridinium salt to the negatively charged dye.

Addition of a  $SiO_2$  colloid to an aqueous solution (pH = 9.3) of the complex  $[Rb^{2+} \cdots MV^{2+}]$  results in the dissociation of the complex. This is evidenced by restoring the absorption spectrum (Figure 3) and fluorescence properties of the free dye upon addition of the  $SiO_2$  colloid. The silanol groups at the surface of the  $SiO_2$  particles are partially ionized at pH = 9.3. Consequently, the colloid particles are negatively charged and exhibit a surface potential of -170 mV.<sup>22b,31</sup> Thus, the separation of the  $[Rb^{2+} \cdots MV^{2+}]$  complex by the  $SiO_2$  colloid is attributed to electrostatic interactions between the complex components and the microheterogeneous environment. The positively charged electron acceptor component,  $MV^{2+}$ , is attracted by the  $SiO_2$  interface while the negatively charged component,  $Rb^{2+}$ , is repelled by it. As a result of the selective association of  $MV^{2+}$  to the colloid particles, the complex is separated and the original photophysical properties

(31) (a) *The Chemistry of Silica*; Iler, R. K., Ed.; Wiley: New York, 1979. (b) *The Electrical Double Layer Around a Spherical Colloid Particle*; Loeb, A. L., Overbeek, J. T. G., Wiersema, P. H., Eds.; M.I.T. Press: Cambridge, MA, 1961.

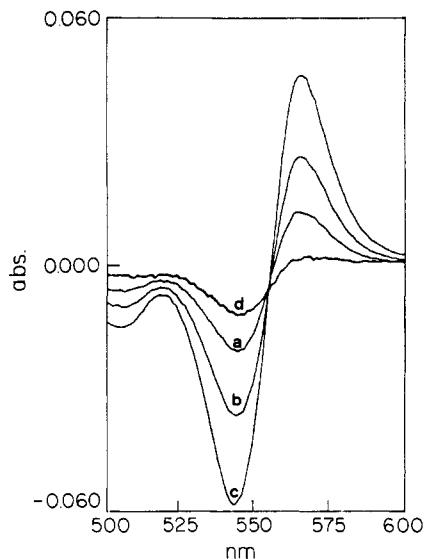


**Figure 3.** Separation of  $[Rb^{2+} \cdots MV^{2+}]$  complex. Differential absorption spectra of rose bengal ( $5 \times 10^{-6}$  M) in the presence of methylviologen: (a)  $1.06 \times 10^{-5}$ , (b)  $2.1 \times 10^{-5}$ , (c)  $4.2 \times 10^{-5}$ , and (d)  $4.2 \times 10^{-5}$  M, with added 0.15% w/w  $SiO_2$  colloid.

**TABLE I: Effect of Ionic Strength on the Photosensitized Reduction of  $MV^{2+}$  in the Microheterogeneous  $SiO_2$  Photosystem<sup>a</sup>**

[NaCl], M	$\psi_s$ , <sup>b</sup> mV	$\Phi$	$k_b$ , <sup>c</sup> $M^{-1} \cdot s^{-1}$	% free dye
0	-170	0.10	$6.4 \times 10^8$	$\approx 100$
0.005	-98	0.034	$1 \times 10^9$	95.1
0.01	-89	0.027	$9 \times 10^9$	91.9
0.05	-69	0.019	$1 \times 10^{10}$	81.4
0.1	-60	0.012	70.1	70.1
no $SiO_2$ colloid		0.0008	$4 \times 10^{10}$	8.3

<sup>a</sup>In all systems  $[Rb^{2+}] = 1 \times 10^{-5}$  M,  $[MV^{2+}] = 1 \times 10^{-3}$  M, and  $[TEOA] = 1 \times 10^{-3}$  M;  $SiO_2$  colloid (1% w/w). <sup>b</sup>Calculated by Gouy-Chapman equation (with Stern modification), eq 8. <sup>c</sup>Calculated by the transient decay curves of  $Rb^{3+}$  at  $\lambda = 415$  nm.

of the dye are restored. We confirmed that electrostatic interactions induced by the  $SiO_2$  colloid are operative in the separation of the complex by altering the ionic strength of the colloid medium. The surface potential of the  $SiO_2$  colloid is strongly affected by the ionic strength of the medium.<sup>31</sup> The effect of ionic strength on the colloid surface potential,  $\psi_s$ , is expressed by the Gouy-Chapman equation (with Stern's modification), eq 8, where  $\sigma_s$

$$\sigma_s = \left[ \frac{2DRT}{\pi} \right]^{1/2} C^{1/2} \sinh \left[ \frac{F\psi_s}{2RT} \right] \quad (8)$$

is the charge density,  $\psi_s$  the surface potential,  $D$  the dielectric constant,  $C$  the total molar concentration of the electrolyte,  $F$  the Faraday constant,  $R$  the gas constant, and  $T$  the absolute temperature. Thus, the surface potential of the  $SiO_2$  colloid decreases as the ionic strength of the environment increases. Consequently, if separation of the  $[Rb^{2+} \cdots MV^{2+}]$  complex by the  $SiO_2$  colloid operates through electrostatic interactions, we anticipate that the effectiveness of the complex separation by the colloid should decrease as the ionic strength of the medium increases. Namely, since addition of the salt reduces the surface potential of the colloid particles, the electrostatic interactions between the microheterogeneous system and the complex components are weakened and the effectiveness of the complex dissociation is reduced.

Table I shows the effect of added salt on the surface potential of the  $SiO_2$  colloid and the effects on the separation efficiency of the  $[Rb^{2+} \cdots MV^{2+}]$  complex. Without added salt the surface potential of the colloid corresponds to -170 mV, and a complete separation of the complex is effected. At a salt concentration of  $[NaCl] = 0.1$  M, the surface potential of the  $SiO_2$  is reduced to -60 mV and only 70% of the complex is separated, implying that electrostatic interactions are operative in the separation of the complex  $[Rb^{2+} \cdots MV^{2+}]$ .

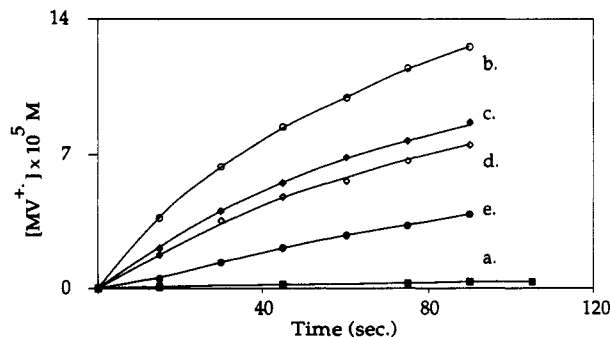
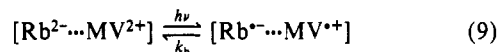


**Figure 4.** Rate of  $MV^{2+}$  formation at time intervals of illumination. All systems included rose bengal ( $1 \times 10^{-5}$  M), TEOA ( $1 \times 10^{-3}$  M), and  $MV^{2+}$  ( $1 \times 10^{-3}$  M), pH = 9.3: (a) in homogeneous solution; (b) in the presence of 1% w/w  $SiO_2$  colloid; (c) with added salt,  $[NaCl] = 0.005$  M; (d) with added salt,  $[NaCl] = 0.01$  M; (e) with added salt,  $[NaCl] = 0.05$  M.

**Photosensitized Reduction of  $MV^{2+}$  by  $Rb^{2-}$  in the Presence of  $SiO_2$  Colloid.** The possibilities of applying reduced bipyridinium salts as electron carriers for hydrogen evolution,<sup>5,6</sup>  $CO_2$  fixation,<sup>7</sup> and hydrogenation processes<sup>10</sup> in the presence of heterogeneous catalysts, i.e., Pt, Rh, Pd, and Ru, evoke interest in the development of photochemical systems for the reduction of bipyridinium salts. Photoreduction of bipyridinium electron acceptors using transition-metal complexes, i.e.,  $Ru(bpy)_3^{2+}$  or Zn porphyrins, or organic dyes, i.e., acridines, as photosensitizers and in the presence of sacrificial electron donors has been the subject of extensive research activities.<sup>32</sup>

We have examined the photosensitized reduction of  $MV^{2+}$  using  $Rb^{2-}$  as photosensitizer and triethanolamine as sacrificial electron donor. Continuous illumination of this photosystem ( $\lambda > 400$  nm) results in the inefficient reduction of  $MV^{2+}$  to  $MV^{+}$ ,  $\phi = 8 \times 10^{-4}$  (Figure 4a). Thus, although the quenching of the excited dye is effective, due to the dye-electron acceptor complex, the yield of the separated photoproduct is very low. This originates from the rapid recombination of the photoproducts in the encounter cage complex that is stabilized by similar attractive interactions operative in the ground state (eq 9). On the other hand,



illumination of the photosystem composed of  $Rb^{2-}$ ,  $MV^{2+}$ , and triethanolamine in the presence of the  $SiO_2$  colloid (1% w/w) results in the effective photoreduction of  $MV^{2+}$ . Figure 4b shows the rate of  $MV^{+}$  formation at time intervals of illumination in the presence of  $SiO_2$  colloid. The quantum yield for  $MV^{+}$  formation corresponds to  $\phi = 1 \times 10^{-1}$  and is ca. 125-fold higher than the quantum efficiency in the homogeneous photosystem that lacks the microheterogeneous environment. It is evident that separation of the ground-state photosensitizer-electron acceptor complex,  $[Rb^{2-} \cdots MV^{2+}]$ , affects the effective photoreduction of  $MV^{2+}$ . Further experiments that examine the effects of ionic strength on the rate of  $MV^{+}$  formation in the presence of the  $SiO_2$  colloid (Figure 4c-e) emphasize the significance of dissociating the ground-state complex to obtain effective reduction of  $MV^{2+}$ . It is evident that as the ionic strength of the system increases, the rate of  $MV^{2+}$  reduction in the presence of the  $SiO_2$  colloid declines. These results are consistent with our previous observations where increase of ionic strength reduced the capability of the  $SiO_2$  to separate the photosensitizer-relay complex. We thus conclude that the formation of the ground-state  $[Rb^{2-} \cdots MV^{2+}]$  complex is destructive toward the reduction of  $MV^{2+}$  (eq 9), but its separation by the microheterogeneous  $SiO_2$  colloid leads to a subsequent effective photoreduction of  $MV^{2+}$ .

To account for the effective photoreduction of  $MV^{2+}$  in the presence of the  $SiO_2$  colloid, we have characterized the photo-

(32) (a) Kalyanasundaram, K. *Coord. Chem. Rev.* **1982**, *46*, 159. (b) Harriman, A.; Porter, G.; Richoux, M.-C. *J. Chem. Soc., Faraday Trans. 2* **1981**, *77*, 833. (c) Kalyanasundaram, K.; Dung, D. *J. Chem. Phys.* **1980**, *84*, 2551. (d) Krasna, A. I. *Photochem. Photobiol.* **1979**, *29*, 267.

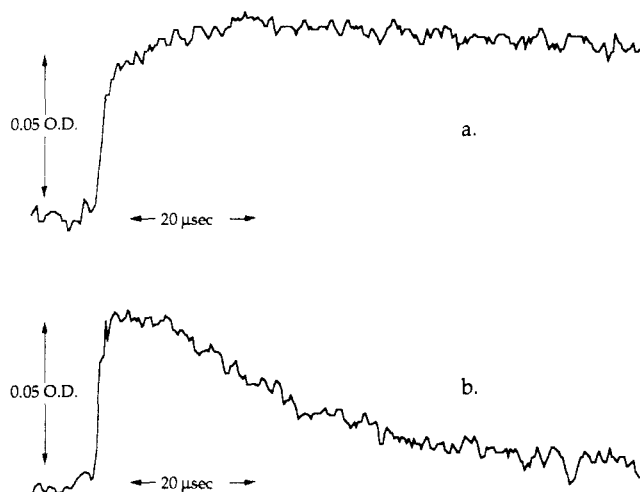
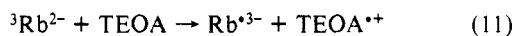
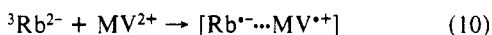
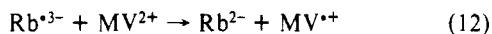


**Figure 5.** Transient decay of semireduced rose bengal,  $\text{Rb}^{3-}$  to  $\text{Rb}^{2-}$  followed at  $\lambda = 415 \text{ nm}$  ( $[\text{Rb}^{2-}] = 1 \times 10^{-5} \text{ M}$ ;  $[\text{TEOA}] = 1 \times 10^{-3} \text{ M}$ ): (a) in aqueous 1% w/w  $\text{SiO}_2$  colloid,  $\text{pH} = 9.3$ ; (b) with added methylviologen,  $1 \times 10^{-3} \text{ M}$ ,  $\text{pH} = 9.3$ .

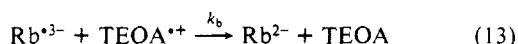
physical properties of  $\text{Rb}^{2-}$  as well as the sequential electron-transfer process in the microheterogeneous system by means of laser flash photolysis. The triplet lifetime of  $\text{Rb}^{2-}$  in a homogeneous aqueous phase ( $\text{pH} = 9.3$ ) is  $\tau = 61 \mu\text{s}$ . In the presence of the  $\text{SiO}_2$  colloid (1%) the lifetime of the excited triplet state is slightly shortened to the value  $\tau = 43 \mu\text{s}$ . Quenching experiments reveal that the triplet excited  $\text{Rb}^{2-}$  is quenched by  $\text{MV}^{2+}$  (eq 10), as well as by TEOA (eq 11), in the microheterogeneous  $\text{SiO}_2$  assembly. The quenching rate constants of triplet  $\text{Rb}^{2-}$  by  $\text{MV}^{2+}$  and TEOA are  $1.18 \times 10^7$  and  $2.9 \times 10^7 \text{ M}^{-1}\cdot\text{s}^{-1}$ , respectively. The oxidative quenching process of the triplet  $\text{Rb}^{2-}$  by  $\text{MV}^{2+}$  (eq 10) does not yield any transient photoproducts, presumably due to rapid back electron transfer in the encounter cage complex of photoproducts. Reductive quenching of triplet  $\text{Rb}^{2-}$  by TEOA (eq 11) is kinetically favored over the oxidative



process and indeed leads to separated photoproducts. The reduced dye,  $\text{Rb}^{3-}$ , is thermodynamically capable of reducing  $\text{MV}^{2+}$  [ $E^\circ(\text{Rb}^{3-}/\text{Rb}^{2-}) = -0.6 \text{ V}$ ;  $E^\circ(\text{MV}^{*+}/\text{MV}^{2+}) = 0.42 \text{ V}$ ], and thus the dark reduction of the electron acceptor (eq 12) follows the primary electron-transfer process. Figure 5a shows the transient absorbance of  $\text{Rb}^{3-}$  (followed at  $\lambda = 415 \text{ nm}$ ), formed upon flashing the dye in the presence of TEOA. Figure 5b shows the transient absorbance of the reduced dye,  $\text{Rb}^{3-}$ , formed upon flashing the photosensitizer in the presence of TEOA and added  $\text{MV}^{2+}$ . We see that in the presence of  $\text{MV}^{2+}$  a rapid decay of the reduced dye occurs ( $k_{\text{obs}} = 3.4 \times 10^7 \text{ M}^{-1}\cdot\text{s}^{-1}$ ). The decay of the reduced dye is thus attributed to the reduction of the electron acceptor,  $\text{MV}^{2+}$ , by  $\text{Rb}^{3-}$  (eq 12).



We note that the photoproducts formed in the primary electron-transfer quenching process (eq 11) exhibit opposite electric charges. Thus, we anticipate that the charged microheterogeneous system will electrostatically interact with the photoproducts: the oxidized photoproduct,  $\text{TEOA}^{*+}$ , will be attracted by the  $\text{SiO}_2$  interface, while the reduced photoproduct,  $\text{Rb}^{3-}$ , will be repelled by the interface. Such electrostatic interactions could significantly effect the recombination of the intermediate primary photoproducts (eq 13). As the reduced photoproduct is repelled by the



colloid interface, the back-electron-transfer reaction of the intermediate photoproducts is anticipated to be retarded. Figure 6a shows the transient absorbance of  $\text{Rb}^{3-}$  in the microhetero-

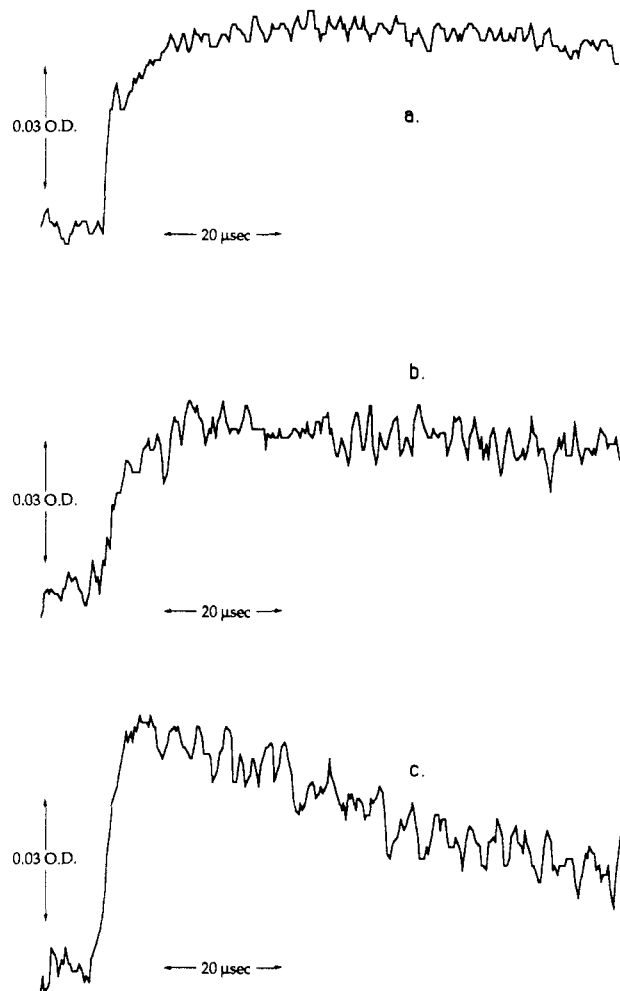


**Figure 6.** Transient decay of semireduced rose bengal,  $\text{Rb}^{3-}$  to  $\text{Rb}^{2-}$  followed at  $\lambda = 415 \text{ nm}$  ( $[\text{Rb}^{2-}] = 1 \times 10^{-5} \text{ M}$ ;  $[\text{TEOA}] = 1 \times 10^{-3} \text{ M}$ ): (a) in the presence of 1% w/w  $\text{SiO}_2$  colloid,  $\text{pH} = 9.3$ ; (b) with added salt,  $[\text{NaCl}] = 5 \times 10^{-2} \text{ M}$ ,  $\text{pH} = 9.3$ ; (c) in a homogeneous aqueous solution,  $\text{pH} = 9.3$ .

geneous  $\text{SiO}_2$  system. The decay curve represents the back-electron-transfer process with the oxidized photoproduct. The bimolecular back-electron-transfer rate constant corresponds to  $k_b = 6.4 \times 10^8 \text{ M}^{-1}\cdot\text{s}^{-1}$ . Figure 6b shows the effect of added salt on the transient decay of  $\text{Rb}^{3-}$  in the microheterogeneous system. The recombination rate constant at  $[\text{NaCl}] = 5 \times 10^{-2} \text{ M}$  is  $1 \times 10^{10} \text{ M}^{-1}\cdot\text{s}^{-1}$  and is 1.6-fold higher than the recombination rate in the absence of added salt. For comparison, the decay curve of  $\text{Rb}^{3-}$  with TEOA $^{*+}$  in a homogeneous phase is given in Figure 6c and corresponds to a recombination rate constant  $k_b = 4.0 \times 10^{10}$ . We thus conclude that the recombination process of the photoproducts is also controlled by means of the  $\text{SiO}_2$  colloid: The negatively charged microheterogeneous interface attracts the oxidized photoproduct while the reduced photoproduct is repelled by the colloid interface. These selective electrostatic interactions retard the back-electron-transfer rate and stabilize the photoproducts against recombination. Consequently, the subsequent reduction of  $\text{MV}^{2+}$  by  $\text{Rb}^{3-}$  (eq 12) competes effectively with the back-electron-transfer process. The effect of added salt on the recombination rate constants highlights the importance of these electrostatic interactions in controlling the back-electron-transfer process. At high ionic strength the surface potential of the  $\text{SiO}_2$  colloid is reduced, and therefore the electrostatic attractive/repulsive interactions with the photoproducts are weakened. This leads to enhanced back electron transfer of the primary photoproducts.

Table I summarizes the quantum yields of  $\text{MV}^{*+}$  formation under steady continuous illumination, the percentage of free photosensitizer, and the recombination rate constants of the

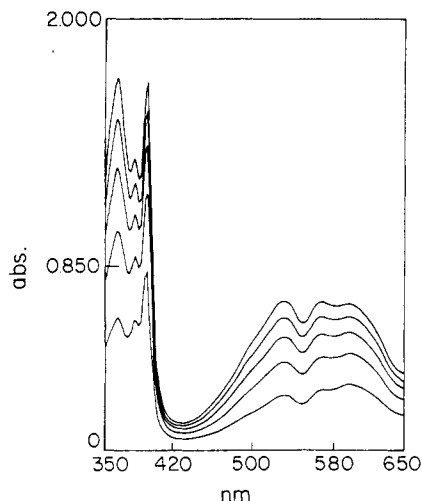
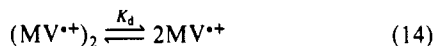


**Figure 7.** Absorption spectra of the photoproducts of  $MV^{2+}$  obtained at 15-s time intervals of illumination of an aqueous solution containing 1% w/w  $SiO_2$  colloid, pH = 9.3.  $[Rb^{2+}] = 1 \times 10^{-5}$  M;  $[TEOA] = 1 \times 10^{-3}$  M.

primary photoproducts in the microheterogeneous  $SiO_2$  photo-system that includes different concentrations of added salt. The surface potential of the  $SiO_2$  colloid in the different systems is also provided. It is evident that as the ionic strength of the system increases, the surface potential of the colloid decreases. We also note that as the surface potential of the colloid is reduced, the quantum yield for  $MV^{2+}$  formation decreases, the percentage of separated photosensitizer from the ground-state  $[Rb^{2+} \cdots MV^{2+}]$  complex is reduced, and the recombination rate constant of the primary photoproducts is enhanced. Thus, we conclude that the microheterogeneous  $SiO_2$  system provides two important complementary functions in controlling the photosensitized reduction of  $MV^{2+}$  in the photosystem that includes  $Rb^{2+}$  as photosensitizer: (i) It effects the separation of the ground-state complex  $[Rb^{2+} \cdots MV^{2+}]$ . Separation of this complex occurs through selective electrostatic interactions between the charged colloid interface and the complex components. The separation of the complex eliminates internal cage recombination and allows charge separation. (ii) The charged  $SiO_2$  colloid stabilizes the primary photoproducts against back-electron-transfer reactions through the selective repulsion of the reduced photoproduct from the colloid interface that attracts the positively charged oxidized products. These two functions complement one another in effecting the high quantum yield for  $MV^{2+}$  in the microheterogeneous environment.

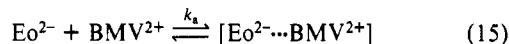
A further aspect to consider involves the distribution of the reduced product,  $MV^{+}$ , in the microheterogeneous  $SiO_2$  system. The reduced product is positively charged and thus is anticipated to be associated with the colloid interface. Figure 7 shows the spectral properties of the reduced product at time intervals of illumination. Interestingly, the absorbance spectra of the photogenerated products are composed of bands at  $\lambda = 394$  and 602 nm characteristic of  $MV^{+}$  and an additional band at  $\lambda = 366$  nm. This latter band has been previously ascribed<sup>33</sup> to a dimer aggregate of  $MV^{+}$ ,  $(MV^{+})_2$ . In a homogeneous aqueous phase aggregation is observable only at high concentration of the monomer radical. The equilibrium constant for the aggregation process has the value  $K_d = 385 \text{ M}^{-1}$ <sup>34</sup> (eq 14). We realize that



aggregation of the reduced photoproduct to form the dimer  $(MV^{+})_2$  indeed occurs in the microheterogeneous system. The aggregation originates from electrostatic association of the reduced photoproduct at the negatively charged  $SiO_2$  interface. This results in a nonuniform distribution of  $MV^{+}$  in the microheterogeneous system, and the high local concentration of  $MV^{+}$  at the colloid

interface effects the dimerization process. From the dimerization equilibrium constant and the absorbance of the dimer band at  $\lambda = 366$  nm, we estimate that the mean concentration of  $MV^{+}$  in the diffuse double layer of the  $SiO_2$  colloid is 0.12 M. The  $MV^{+}$  attracted by the  $SiO_2$  colloid is not in geminate contact with the negatively charged groups of the  $SiO_2$  colloid. We view the concentration of  $MV^{+}$  at the  $SiO_2$  interface as a diffuse double layer in the vicinity of charged colloid particles.<sup>30b</sup> The production of localized, highly concentrated regions of the reduced photoproduct in the microheterogeneous system might be of substantial value for subsequent catalytic transformations. Immobilization of metal catalysts onto the  $SiO_2$  colloid and localization of the reduced photoproduct at the colloid interface provide an organized assembly for effective sequential catalytic electron-transfer processes.

**Eosin Photosensitized  $H_2$  Evolution from the Microheterogeneous  $SiO_2$  Colloid.** The  $SiO_2$  colloid operates in controlling the photosensitized reduction of bipyridinium relay compounds by xanthene dyes in basic aqueous media (pH > 9). To effect  $H_2$  evolution at this pH the reduced relay should exhibit a reduction potential of  $E^\circ = -0.531$  V vs NHE as a thermodynamic requirement. *N,N'*-Dimethyl-4,4'-bipyridinium radical cation,  $MV^{+}$ , does not exhibit the corresponding reduction potential ( $E^\circ(MV^{+}/MV^{2+}) = -0.42$  V), and thus its application in this system as electron-transfer mediator for  $H_2$  evolution should be excluded. We have designed an approach to tailor the reduction potentials of viologen type electron acceptors by means of substituents of steric hindrance in positions 3 and 3' of the bipyridinium backbone. Steric hindrance in positions 3 and 3' is anticipated to distort the two pyridinium rings from planarity.<sup>35</sup> Upon reduction of the bipyridinium array, the two rings are forced, however, to a planar configuration to maintain effective  $\pi$ - $\pi$  overlap and resonance delocalization. Thus, bulky substituents at positions 3 and 3' of the bipyridinium salt introduce steric hindrance for the planar conformation, and consequently the reduction process of the bipyridinium salt is more difficult. Namely, the reduced photoproduct should exhibit a more negative reduction potential as compared to the unsubstituted relay. Following this rationale, we have synthesized *N,N'*-dibenzyl-3,3'-dimethyl-4,4'-bipyridinium dibromide,  $BMV^{2+}$  (3), by alkylation of 3,3'-dimethyl-4,4'-bipyridine with benzyl bromide. The reduction potential of  $BMV^{2+}$  corresponds to  $E^\circ(BMV^{+}/BMV^{2+}) = -0.670$  V vs NHE. For comparison, the reduction potential of *N,N'*-dibenzyl-4,4'-bipyridinium,  $BV^{2+}$  (4), is  $E^\circ(BV^{+}/BV^{2+}) = -0.340$  V, implying that steric hindrance in the bipyridinium backbone indeed lowers the reduction potential of the resulting radical. Thus,  $BMV^{2+}$  could act as electron acceptor in microheterogeneous  $SiO_2$  colloids (pH = 9.3), and its reduced photoproduct,  $BMV^{+}$ , is thermodynamically capable of mediating  $H_2$  evolution from this basic environment. Rose bengal in its reduced form,  $Rb^{3-}$ , is, however, not capable of reducing  $BMV^{2+}$  ( $E^\circ(Rb^{3-}/Rb^{2-}) = -0.60$  V vs NHE). Thus, the xanthene dye,  $Rb^{2-}$ , was substituted by eosin Y,  $Eo^{2-}$  (5), which exhibits in its reduced form a proper thermodynamic potential to reduce  $BMV^{2+}$ ,  $E^\circ(Eo^{3-}/Eo^{2-}) = -0.8$  V vs NHE.<sup>36</sup> Eosin,  $Eo^{2-}$  (5), forms a ground-state complex with  $BMV^{2+}$  (eq 15). The association



constant of the complex  $[Eo^{2-} \cdots BMV^{2+}]$  has been determined spectroscopically and by fluorescence quenching to have the value  $K_a = 17000 \pm 3400 \text{ M}^{-1}$ . The complex is separated by the  $SiO_2$  colloid through selective association of 3 to the colloid interface and concomitant repulsion of the xanthene dye. Illumination of an aqueous  $SiO_2$  colloid that includes eosin,  $Eo^{2-}$ , as photosensitizer,  $BMV^{2+}$  as electron acceptor, and TEOA as sacrificial electron donor results in the formation of  $BMV^{+}$  through a sequence of reactions outlined in eqs 16 and 17.

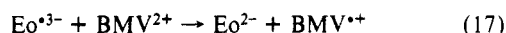
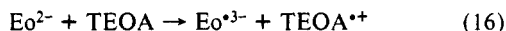
(34) Kosower, E. M.; Cottes, J. L. *J. Am. Chem. Soc.* **1964**, *86*, 5224.

(35) (a) Hunig, S.; Gross, J.; Schenk, W. *Justus Liebig's Ann. Chem.* **1973**,

324. (b) Hunig, S.; Gross, J. *Tetrahedron Lett.* **1968**, 2599.

(36) Moser, J.; Grätzel, M. *J. Am. Chem. Soc.* **1984**, *106*, 6557.

(33) Neta, P.; Richoux, M.-C. *J. Chem. Soc., Faraday Trans. 2* **1985**, *81*, 1427.

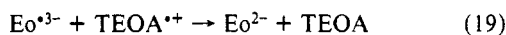


To design the photocatalytic microheterogeneous assembly for  $\text{H}_2$  evolution, immobilization of a metal catalyst onto the  $\text{SiO}_2$  colloid is desired. Illumination of an aqueous  $\text{SiO}_2$  colloid that includes  $\text{Eo}^{2-}$  as photosensitizer,  $\text{BMV}^{2+}$  as electron acceptor, and TEOA as sacrificial electron donor in the presence of  $\text{Pd}^{2+}$  ions ( $1.3 \times 10^{-6}$  M  $\text{Pd}(\text{NO}_3)_2$ ) results in the formation of a brown colloid and concomitant  $\text{H}_2$  evolution from the system. The rate of  $\text{H}_2$  evolution from the system is displayed in Figure 8. The brown colloid formed upon illumination of the system was dialyzed after  $\text{H}_2$  evolution commenced, and the resulting colloid was analyzed by electron microscopy. The TEM picture of the colloid reveals that the  $\text{SiO}_2$  particles (40–70-Å diameter) are covered with dark spots and often several  $\text{SiO}_2$  particles aggregate around a dark catalyst site. No separated free dark particles are detected in the TEM. Electron dispersion spectroscopic analysis of the particles shows that the dark spots are composed of Pd. Thus, the Pd catalyst is immobilized onto the  $\text{SiO}_2$  particles upon illumination of the photosystem. The selective immobilization of the metal catalyst (Pd) on the  $\text{SiO}_2$  particles originates from electrostatic attraction of  $\text{Pd}^{2+}$  ions to the microheterogeneous interface. The reduced photoproduct formed upon the photosensitized electron-transfer process,  $\text{BMV}^{*+}$ , reduces the  $\text{Pd}^{2+}$  associated with the  $\text{SiO}_2$  surface (eq 18) and results in the micro-



heterogeneous catalytic assembly. Introduction of the dialyzed  $\text{SiO}_2$ -Pd colloid into an aqueous photosystem that includes  $\text{Eo}^{2-}$ , the electron acceptor,  $\text{BMV}^{2+}$ , and TEOA results, upon illumination, in  $\text{H}_2$  evolution, implying that the colloid composed of Pd deposited onto  $\text{SiO}_2$  acts as the  $\text{H}_2$  evolution catalyst.

In view of the previous discussion, the effect of the Pd/ $\text{SiO}_2$  colloid on  $\text{H}_2$  evolution can be summarized as follows: The  $\text{SiO}_2$  colloid effects, by means of electrostatic interactions, the separation of ground-state eosin-relay complex (eq 15) and subsequently retards the recombination rate of the photogenerated photoproducts (eq 19). The stabilization of the photoproducts against back electron transfer allows the effective formation of  $\text{BMV}^{*+}$  which mediates  $\text{H}_2$  evolution in the presence of the  $\text{Pd}^0$  catalyst (eq 20).



The mechanism of  $\text{H}_2$  evolution at metal interfaces has been extensively explored. It involves the primary charging of the metal with electrons transferred by the reduced relay.<sup>37</sup> The charged metal, acting as electron sink, reduces protons to form metal bound H atoms. Dimerization of hydrogen atoms at the metal surface leads to  $\text{H}_2$  evolution. Kinetic studies have indicated that the dimerization of hydrogen atoms on the metal surface is a relatively slow process.<sup>10,37</sup> Thus, in the presence of a substrate that utilizes effectively the metal bound H atoms, hydrogenation of the sub-

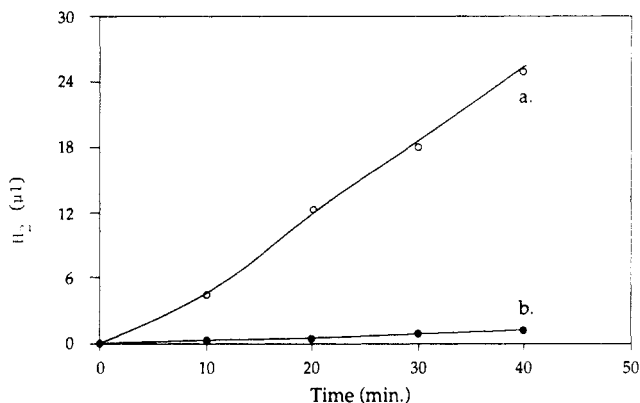


**Figure 8.** Rate of hydrogen production at time intervals of illumination of aqueous systems containing eosin Y ( $1 \times 10^{-5}$  M), TEOA ( $1 \times 10^{-3}$  M), and  $\text{BMV}^{2+}$  ( $1 \times 10^{-3}$  M), pH = 9.3: (a) in the presence of 1% w/w  $\text{SiO}_2$  colloid; (b) in a homogeneous solution.

strate competes with the  $\text{H}_2$  evolution process. This characteristic of the  $\text{H}_2$  evolution process has been applied in the photoinduced hydrogenation of unsaturated substrates and hydrogenation of  $\text{HCO}_3^-$  to formate. We find that the microheterogeneous  $\text{SiO}_2$ -Pd assembly that includes  $\text{Eo}^{2-}$  as photosensitizer,  $\text{BMV}^{2+}$  as electron acceptor, and TEOA as sacrificial electron donor can be similarly applied for the effective hydrogenation of ethylene. Illumination of this photosystem in the presence of ethylene results in the effective formation of ethylene ( $\text{C}_2\text{H}_4$ ),  $\phi = 1.1 \times 10^{-3}$ , and no  $\text{H}_2$  evolution occurs. The effective formation of ethane is attributed to hydrogenation of ethylene by "in situ" generated Pd-H species, a process that competes with the  $\text{H}_2$  evolution process.

## Conclusions

Xanthene dyes form ground-state dye-bipyridinium complexes that eliminate the application of these dyes as photosensitizers for the photoreduction of bipyridinium electron acceptors. A microheterogeneous  $\text{SiO}_2$  colloid provides an organized microenvironment for controlling the photosensitized reduction of bipyridinium electron acceptors with xanthene dyes. (i) The microheterogeneous assembly separates the ground-state dye-electron acceptor complex by the selective attraction of the positively charged complex component to the colloid interface. (ii) The microheterogeneous system provides a means to stabilize the photoproducts against back-electron-transfer reactions, and (iii) it localizes the reduced photoproduct at the colloid interface. These functions lead to the effective photoreduction of the bipyridinium salts.

We have also revealed photochemical means for the immobilization of metal catalyst onto  $\text{SiO}_2$  colloids. Concentration of the reduced electron acceptor at the colloid-metal interface, through electrostatic interactions, provides an organized catalytic assembly for  $\text{H}_2$  evolution and photohydrogenation processes.

**Acknowledgment.** This research was supported by The Fund for Basic Research administered by The Israel Academy of Sciences and Humanities.

(37) Willner, I.; Mandler, D. *J. Am. Chem. Soc.* **1989**, *111*, 1330.